manuscript accepted for publication by *JGR: Planets*

Instantaneous habitable windows in the parameter space of Enceladus' ocean

Peter M. Higgins[1,2], Christopher R. Glein[3], and Charles S. Cockell[1]

[1]UK Centre for Astrobiology, School of Physics and Astronomy, University of Edinburgh, Edinburgh, UK
[2]Institute for Astronomy, Royal Observatory, Blackford Hill, Edinburgh, UK
[3]Space Science and Engineering Division, Southwest Research Institute, San Antonio, TX, USA

Key Points:

- Key known drivers of the Enceladus ocean's habitability with respect to methanogens are identified and their uncertainties accounted for.
- There is energy available for methanogens in most cases if the pH of the bulk ocean is less than 10.
- Instantaneous microbial power supplies imply both habitable and uninhabitable conditions are possible.

Corresponding author: Peter M. Higgins, p.m.higgins@ed.ac.uk

Abstract

In recent years, Enceladus' subsurface ocean has become a tantalising case-study for potentially habitable conditions in an extraterrestrial ocean world. However, we still know very little about its subsurface conditions. Its oceanic composition is difficult to characterise with current data and estimates are highly dependent on model-based interpretations which are also not yet tightly constrained. In light of these uncertainties, we consider a wide selection of the inferred parameter spaces to quantify the energy available to putative hydrogenotrophic methanogens on Enceladus in the bulk ocean at cool and elevated temperatures. We estimate the instantaneous power supply their metabolism could provide in these conditions and compare it to expected power demands of life on Earth. To be habitable for methanogens a 273 K ocean with relatively high salt content must have pH<10, and a relatively low salt ocean must have pH<8 at 273 K, or pH<9 when heated to >360 K. Some combinations meet the power demands of exponential growth, but large swathes of the parameter space appear energetically uninhabitable. The habitability of the Enceladus ocean for methanogens appears to be a delicate balance between its temperature, pH, salinity and concentrations of carbonates, nutrients and dissolved gases (particularly H_2). Many of these parameters are co-dependent; variation in any one of them could tip the balance into uninhabitable conditions. Further constraining these variables should be a priority for future missions to ocean worlds in order to enable definitive assessments of their habitability.

Plain Language Summary

Observations of Enceladus in recent years have revealed tantalising details of its potentially habitable subsurface ocean, allowing its conditions to be resolved in unprecedented detail compared to other icy moons. Still, the variation in possible parameters below its icy shell is huge, ranging from the cold bulk ocean with a pH similar to seawater on Earth to potentially scalding alkaline fluids at its depths. The ocean contains the ingredients of an ancient metabolism which is used by life on Earth by organisms known as methanogens. In this work, we explore the instantaneous habitability of Enceladus' subsurface ocean to methanogens using a range of environmental parameters informed by data from the Cassini mission and modelling. In other words, we ask: if Cassini's observations offered a 'snapshot' view of the ocean, does a habitable window exist within the uncertainty of the data, without considering as-yet unconstrained (but still important) variables such as a supply of nutrients? Some parameter combinations appear habitable, but not all the combinations are suitable for methanogens as we know them on Earth. We identify the most important drivers of habitability in Enceladus' ocean and explain how they can be better constrained by future research or space missions.

1 Introduction

Enceladus is a unique and important target for astrobiology in the solar system. The icy moon has a large subsurface ocean (Iess et al., 2014; Thomas et al., 2016), and analysis of measurements by the Cassini mission show the existence of CO_2, H_2, and CH_4 — the reactants and products of the hydrogenotrophic methanogenesis metabolism — as well as salts, silica and organics (e.g. Waite et al., 2009; Bouquet et al., 2015; Waite et al., 2017; Postberg et al., 2009, 2018; Hsu et al., 2015). These species were detected in plumes of gases and ice grains which erupt from Enceladus' south polar region. Determining the exact oceanic composition of these species from plume data has proven difficult. Estimates extend over many orders of magnitude and are strongly coupled to pH (Waite et al., 2017; Glein & Waite, 2020), which is not well-constrained itself. Estimates of oceanic pH range between 8–13.5 with most

studies settling on the weakly-alkaline end of this scale (e.g. Postberg et al., 2009; Hsu et al., 2015; Glein et al., 2015; Glein & Waite, 2020).

From the Cassini data there is limited information about the icy moon's subsurface ocean, but comparisons have been drawn to inhabited Earth systems such as sub-glacial lakes and alkaline hydrothermal vents (e.g. Jones et al., 2018). There is overlap in Enceladus' possible parameter space with those environments in which methanogens are known to grow and reproduce on Earth (Taubner et al., 2015). Enceladus' subsurface ocean has hence become a compelling target for geochemical and astrobiological modelling analyses (e.g. Waite et al., 2017; Glein et al., 2015; Glein & Waite, 2020; Steel et al., 2017; Ray et al., 2021; H. B. Smith et al., 2020; Cable et al., 2020; Affholder et al., 2021).

Estimates of the icy moon's composition have been used to explore whether there is sufficient energy available to sustain life (e.g. Waite et al., 2017; Steel et al., 2017; Ray et al., 2021). This is achieved by estimating the Gibbs free energy ΔG [J mol^{-1}] of potential metabolic pathways, a measure of the energy that life can extract from chemical disequilibrium in an environment. These assessments are limited however because they depend upon the weakly constrained physico-chemical conditions in the ocean (Hendrix et al., 2018). Waite et al. (2017) identified that in the bulk ocean there is Gibbs free energy available through hydrogenotrophic methanogenesis and since then it has widely been assumed that there is energy for life on Enceladus. However, this is not conclusive evidence that the subsurface ocean is habitable. A more comprehensive picture requires 1) a wider parameter space, accounting for various expected temperatures, pressures, salinities, pH values and other relevant physico-chemical parameters; and 2) consideration of the thermodynamics and kinetics of microbial metabolism to assert whether the available energy could be biologically useful in those settings.

One way to assess habitability quantitatively is by computing the energy fluxes available to life (power supply) and comparing them to the energetic demands posed by its environment (maintenance, or power demand) (Hoehler, 2007). The power supply can be determined from a combination of the available ΔG from a potential metabolic pathway — which is determined by the temperature, pressure and chemical composition — and kinetic factors related to the organism and its environment (Higgins & Cockell, 2020). The power demand reflects the energetic cost of processes necessary for survival but not strictly related to growth. These could include the burdens of biomass degradation at elevated temperatures and pressures, or the toll of maintaining a consistent internal pH and cell composition at adverse pH and salinity, for example (Hoehler, 2007). The maintenance power also varies with the growth state of the organism (Hoehler & Jørgensen, 2013).

In this work, we examine the instantaneous habitability of Enceladus' subsurface ocean to hydrogenotrophic methanogens using a wide parameter space informed by Cassini data and modelling. This allows us to initially assess whether the ocean could be habitable based on observed parameters, at an instant in time, without requiring energy and nutrient inflows. We use a geochemical model coupled to a bioenergetic model to predict how the ranges of temperature, pressure, pH, salt content, and dissolved gas composition affect the ocean's habitability to Earth-like methanogens. This assessment is performed by first calculating the free energy yield of hydrogenotrophic methanogenesis, converting it to a microbially accessible power supply and comparing that to 1) typical maintenance powers and 2) known power supplies and demands associated with methanogens and other anaerobes on Earth.

2 Methods

The bioavailable power supply is determined by both the degree of energy availability in a system and an organism's ability to utilize that energy. These are governed by a combination of environmental (e.g. composition, temperature) and organismic (e.g. kinetics and energetic yield of metabolism) variables. For this work, a geochemical speciation model was used to estimate the dissolved gas composition and pH of the ocean under a variety of conditions. This was then used as an input to a bioenergetic model to compute the energetic availability and possible power supplies to hydrogenotrophic methanogens.

2.1 Geochemical model

The thermodynamic drive for hydrogenotrophic methanogenesis depends on the activities of CO_2, H_2, CH_4, and H_2O. The activity can be thought of as an effective concentration that is used to quantify relative stability under non-standard conditions. Aqueous species' activities are based on the 1 molal (mole of solute per kg of water) standard state that is referenced to infinite dilution at any pressure and temperature, and the activity of H_2O is relative to the pure solvent.

The activity of CO_2 in Enceladus' ocean was previously estimated by calculating the carbonate speciation at 0 °C (Waite et al., 2017), using the composition of major identified salts (NaCl, $NaHCO_3$ and/or Na_2CO_3) in plume ice grains (Postberg et al., 2009) and a suggested pH range of ∼9–11 (Glein et al., 2018). The activities of H_2 and CH_4 in Enceladus' ocean were estimated by assuming that the number ratios of these species relative to CO_2 in the ocean are similar to those in the plume gas, and also assuming that the activities of neutral species can be approximated by their molal concentrations (Waite et al., 2017). The activity of H_2O was set to unity, as is typical in fluids that are not highly concentrated in salts.

Here, we extend the dissolved gas model of Waite et al. (2017) to elevated temperatures, motivated by the significant interest in hydrothermal environments on Enceladus (Hsu et al., 2015; Choblet et al., 2017; Liao et al., 2020). Such systems (or parts of them) could serve as habitable zones inside Enceladus, so it is important to understand how the thermodynamics of methanogenesis would change at temperatures higher than that of the bulk ocean. To estimate the activities of methanogenesis reaction species above 273 K, we take the inferred ocean composition from Waite et al. (2017) and respeciate the ocean water at different temperatures. This 'heated seawater' approach does not consider that chemical processes in hydrothermal environments such as water-rock interaction will increasingly contribute to the ocean composition in regions of elevated temperature. We do not include an estimate of the hydrothermal fluid composition on Enceladus beyond such heated seawater. However, it is a useful first step and may be relevant to possible Enceladean seawater aquifers and warmer regions of the ocean which are dominated by seawater, discussed further in Section 5. It also allows us to explore what happens in the hypothetical scenario where Enceladus' bulk ocean is heated up, and how this affects its habitability to methanogens.

The respeciation calculations are performed using the SpecE8 app in The Geochemist's Workbench 15, with the thermo.com.V8.R6+ database. This program calculates chemical equilibrium by simultaneously solving all of the equilibrium constant and mass balance relationships among aqueous species (Bethke, 2008) in the simplified Enceladus ocean system of Na–Cl–CO_2–O–H. We represent the composition of dissolved salts in the same way as done by Glein and Waite (2020). The two key model input parameters for the detected salts are the total concentration of chloride [Cl], and the concentration of dissolved inorganic carbon [DIC] (sum of the molalities of CO_2(aq), HCO_3^-(aq) and CO_3^{2-}(aq)). Postberg et al. (2009) provide constraints on [Cl] (0.05–0.2 mol kg^{-1}) but only the sum of bicarbonate and carbonate (0.02–0.1

mol kg^{-1}). Because of this, we had to first find the corresponding [DIC] as a function of ocean pH. Once that value was obtained, SpecE8 was used to compute the concentration of Na via charge balance, and this value was then used to evaluate the pH at elevated temperatures.

At elevated temperatures, the activities of H_2 and CH_4 stay fixed at ocean values in our model because there are no alternative forms of these species (for simplicity, we do not consider redox reactions during the cooling trajectory, but these could be ongoing (discussed in Section 5.2)). In contrast, the activity of CO_2 is allowed to vary because the carbonate speciation changes with temperature. This occurs because the equilibrium constants between carbonate species (e.g., CO_2, HCO_3^-, CO_3^{2-}) are temperature dependent, and the fluid pH co-evolves with the carbonate speciation. The activity of H_2O is also obtained as an output of these calculations.

2.2 Bioenergetic model

The bioenergetic model NutMEG (Higgins, 2021; Higgins & Cockell, 2020) was used to compute Gibbs free energies of methanogenesis, ATP production and the power supply available for methanogens across the Enceladus ocean's parameter space. NutMEG is a Python package for predicting habitability and biomass in environments relevant to astrobiology. It casts microbial behavior in a quantitative framework and considers the power supply available for life in a given environment, the power demands associated with living in such settings, and the availability of key nutrients. In this work NutMEG was used to calculate the instantaneous bioavailable power supplies provided by the parameter space and compare them to the power demands experienced by life on Earth.

In order to compute the available Gibbs free energy, NutMEG requires the environmental temperature T, pressure P, and activities of all metabolic reagents. In addition to these, computing the bioavailable power supply requires a number of organism-specific parameters. These include: the rate constant of the metabolism k at T and P; the net ATP yield n_{ATP} (the number of moles of ATP formed per mole of CO_2 consumed); and the cell composition. These latter variables have been constrained previously for hydrogenotrophic methanogens (Section 3.3, Supplemental Figures S1, S4, S5, Higgins and Cockell (2020)). NutMEG calculates the bioavailable power supply using thermodynamically limited biochemical kinetics, in which the power conserved by life is dependent on both the Gibbs free energy of the overall metabolic reaction and the amount of energy the organism can preserve via ATP production (Jin & Bethke, 2007; Higgins & Cockell, 2020).

For a chemical reaction, the Gibbs free energy ΔG is given by:

$$\Delta G = \Delta G^\circ + RT \ln Q \tag{1}$$

where ΔG° [J mol^{-1}] is the standard Gibbs free energy of the reaction, R [J $(mol\ K)^{-1}$] is the universal gas constant, and Q the reaction quotient, all at temperature T [K] and pressure P [Pa]. Q is calculated from the activities of the reaction species and stoichiometry of the reaction and ΔG° is computed using SUPCRT92 (Johnson et al., 1992) with the slop07 database. This software calculates thermodynamic parameters at a wide range of temperatures and pressures, and slop07 includes many useful biomolecules such as ATP and ADP (LaRowe & Helgeson, 2006). Thermodynamic data for the other chemical species used in this work originates from Shock et al. (1989) and Plyasunov and Shock (2001). NutMEG computes the Gibbs free energy using equation 1 for both the overall metabolism (ΔG_{M}):

$$CO_2 + 4\,H_2 \rightleftharpoons 2\,H_2O + CH_4 \tag{2}$$

and for ATP production ΔG_{ATP}:

$$\mathrm{ADP} + \mathrm{P_i} \rightleftharpoons \mathrm{ATP} + \mathrm{H_2O} \tag{3}$$

where $\mathrm{P_i}$ represents an orthophosphate ion. To carry out these calculations requires the activities of all constituents. We used NutMEG's default configuration for calculating ΔG_{ATP} using values for [ADP], [ATP] and [$\mathrm{P_i}$] which aim to be broadly representative of life on Earth: 0.1, 5 and 4 mmol $\mathrm{L^{-1}}$ respectively (Albe et al., 1990). These concentrations vary significantly between organisms and their metabolic states, but for this work we address this issue by considering a broad range of n_{ATP} values which offer comprehensive coverage of energetic uptake (Section 3.3, Supplemental Figure S4). The temperature dependence of ΔG_{ATP} owes mainly to the temperature dependence of $\Delta G^{\circ}{}_{\mathrm{ATP}}$ (Supplemental Figures S1, S4). Further information on the specific methods employed by the model and the code prepared for this work are summarised in the Supplemental Material, NutMEG's documentation (Data Availability, Higgins (2021)), and by Higgins and Cockell (2020).

3 Parameter space selection

We have deliberately chosen a wide range of parameter values to encompass the uncertainties in the Cassini observational data and current interpretations of these data. This allows us to explore as broad a range of possible values that might exist in Enceladus' ocean, and to take into account the range of environmental parameters under which methanogenesis can occur on Earth. The energetic and power availability in the ocean was computed over a grid of possible temperature and pH values. The chemical composition and microbial parameters were constrained to within expected uncertainties and the total parameter space considered for this analysis is shown in Table 1.

3.1 Temperature and pressure

Enceladus' ocean is thought to have a temperature minimum ≈272 K at the water-ice interface increasing to ≈363 K or a maximum possible ≈563 K at the ocean floor (the boiling limit) (Glein et al., 2018; Hsu et al., 2015). Improved constraints on the hydrothermal temperatures within the core are required to specify the temperatures at which the hydrothermal fluid meets the bulk ocean (e.g. Glein et al., 2018; Hsu et al., 2015; Waite et al., 2017; Choblet et al., 2017), but the temperature difference between the water-ice and water-core boundaries must be at least 90 K (Cable et al., 2020; Hsu et al., 2015; Sekine et al., 2015). The temperatures of putative hydrothermal systems in the core have been inferred from their expected mineralogy and the pH of the ocean as those required to satisfy Cassini observations of silica and $\mathrm{H_2}$ (e.g. Hsu et al., 2015; Choblet et al., 2017; Waite et al., 2017; Glein et al., 2018). For this study, a temperature distribution between 273–473 K was adopted. While this does not increase to the highest suggested temperatures, the current maximum temperature limit observed for life is 395 K (Takai et al., 2008). Also, our heated seawater approach becomes increasingly less accurate at elevated temperatures due to the likely contribution of hydrothermal fluid to the overall composition (discussed in Section 5.2).

The pressure of the ocean is dependent on its depth and the thickness of the surface ice shell. Current estimates suggest the differentiated hydrosphere to have an average thickness of 21 km and 37 km for the shell and the ocean respectively (Hemingway & Mittal, 2019). If at the ocean's deepest point the ice shell is only a few kilometers thick, a widest pressure variability of between ∼1 and ∼100 bar can be expected. This pressure choice has a minimal effect ($\ll$1 kJ $\mathrm{mol^{-1}}$) on ΔG° compared to temperature for both methanogenesis and ATP production (Supplemental Figure

Table 1. Parameter range of Enceladus' ocean and hydrogenotrophic methanogens considered for this study.

Environmental parameter	**Symbol**	**Proposed range**	**Reference(s)**	**Range used**	**Internal dependencies**
Temperature	T	272–563 K	Section 3.1	273–473[a] K	–
Pressure	P	1–100 bar	Section 3.1	1 bar[f]	–
Bulk ocean pH	pH_{bo}	8–13.5	various[b]	7–12	–
Speciated pH[c]	pH	–	various[c]	6.77–12	T, a_{CO2}
Activity of CO_2[c]	a_{CO2}	–	various[c]	10^{-10}–10^{-2}	T, pH_{bo}
Plume volume mixing ratio of CH_4	–	$0.2\% \pm 0.1$	Waite+ 2017	$0.2\% \pm 0.1$	–
Plume volume mixing ratio of H_2	–	$0.9\% \pm 0.5$	Waite+ 2017	$0.9\% \pm 0.5$	–
Dissolved inorganic carbon	[DIC]	0.01–0.1 mol kg^{-1}	Section 2.1	0.01–0.1 mol kg^{-1}	–
Concentration of Cl	[Cl]	0.05–0.2 mol kg^{-1}	Postberg + 2009	0.05–0.2 mol kg^{-1}	–
Organism parameter	**Symbol**	**Proposed range**	**Reference**	**Range used**	**Internal dependencies**
ATP yield per mol CO_2	n_{ATP}	$\leq$2.0	Section 3.3	0.25–2.0	–
$\log_{10}$ methanogenesis rate constant[d]	$\log_{10}(k)^d$	[(−7)–0] $\pm 1^d$	Higgins+ 2020	[(−7)–0] $\pm 1^d$	T, n_{ATP}
Energy of protein synthesis	E_{pro}	–	Higgins+ 2020	790–2750 J (dry g)$^{-1}$	T, organism composition
Methanogen power demand[e]	–	–	Higgins+ 2020	$\sim 10^{-15}$–10^{-9} W cell^{-1}	T, k
Anaerobe power demand[e]	–	–	Tijhuis+ 1993	$\sim 10^{-14}$–10^{-10} W cell^{-1}	T, cell mass
Minimal power demand[e]	–	–	Lever+ 2015	$\sim 10^{-20}$–10^{-12} W cell^{-1}	T, E_{pro}
Minimum Earth power supplies	–	–	Bradley+ 2020	$\sim 10^{-21}$–10^{-18} W cell^{-1}	–

[a] This maximum is variable depending on the geochemistry of rock-water reactions at the bottom of the ocean. The upper temperature limit could be much higher, but 473 K is already well above the known maximum temperature limit for life. See main text for details.
[b] We consider a wider range than recent studies which have constrained the oceans' pH values to 8–10 (see main text).
[c] By the carbonate speciation model used, the activity of CO_2 is estimated from the pH at 273 K. Upon increasing the temperature, the model was internally respeciated to acquire new values of CO_2 activity and pH. These rows do not contain entries for 'expected range' because they were computed for the parameter space as summarized in Section 2.1.
[d] Rate constants calculated in Higgins & Cockell (2020) were based on hydrogenotrophic methanogens in the exponential phase under optimal conditions and vary with temperature as shown in Supplemental Figure S5.
[e] The ranges for the power demands correspond to their values at temperatures between 273 and 400 K rather than the full temperature range of the parameter space. This is because 400 K is an approximate maximum temperature limit for life.
[f] Higher pressures are not considered for reasons outlined in the main text. Differences in output between 1–100 bar are expected to be small in comparison to the effects of other variables in the parameter space (section 3.1, Supplemental Figure S3).

manuscript accepted for publication by *JGR: Planets*

S1), and the pressure effects on life are poorly understood (Meersman et al., 2013; Lauro & Bartlett, 2008). We expect any changes in composition caused by pressure to be insignificant in comparison to those caused by other variables in the parameter space. By computing the equilibrium constants of the carbonate system at 1 and 100 bar, we can expect the activity of CO_2 (a_{CO2}) to vary by 7–25% (Supplemental Figure S3). This variation is negligible when compared to that due to salt content and pH which affect a_{CO2} by orders of magnitude (discussed below). To avoid complications with temperature, depth and the software used for chemical speciation, pressure effects are not considered in this analysis and all calculations were performed at the default value of The Geochemist's Workbench and SUPCRT92 which is 1 bar between 273–373 K and the saturation pressure of H_2O at temperatures higher than this.

3.2 Chemical composition and pH

A number of studies have estimated the pH of Enceladus' ocean and largely agree that it is likely to be weakly to strongly alkaline with pH>8 (Zolotov, 2007; Postberg et al., 2009; Hsu et al., 2015; Glein et al., 2015; Glein & Waite, 2020). In this study, a range of "bulk ocean pH" values (defined as the pH of the ocean at 273 K) between 7 and 12 were used, encompassing most of these estimates. The carbonate speciation model outlined in Section 2.1 was used to compute the activity of CO_2 (a_{CO2}) at 273 K and the specified ocean pH in three scenarios: a high salt, high carbonates case ([Cl]=0.2 mol kg^{-1}, [DIC]=0.1 mol kg^{-1}), a low salt, low carbonate case ([Cl]=0.05 mol kg^{-1}, [DIC]=0.01 mol kg^{-1}) and a nominal case ([Cl]=0.1 mol kg^{-1}, [DIC]=0.03 mol kg^{-1}). These maximise, minimise and provide the geometric mean for a_{CO2} respectively which are consistent with Cassini data (Supplemental Table S1, Supplemental Dataset, Glein & Waite, 2020).

To account for the changing pH and a_{CO2} with seawater temperature, the speciation was performed on the ocean solution again after heating the fluid by intervals of 10 K. In other words, the simulated solution was warmed and its pH, water activity (a_{H2O}) and a_{CO2} were self-consistently recalculated at the new temperature. The effect this has on the pH is shown by the dashed lines in Figure 1. Its uncertainty and effect on a_{CO2} can be found in the Supplemental Dataset and is visualized in Supplemental Figure S2.

The activities of H_2 (a_{H2}) and CH_4 (a_{CH4}) and their uncertainties were calculated by comparison between their volume mixing ratios reported by Cassini (Table 1, Waite et al. (2017)) and that of CO_2 which is 0.55 % $\pm$ 0.25 using the CO_2 activity calculated at 273 K. It was assumed that a_{H2} and a_{CH4} are unaffected by the ion speciation, and do not significantly change with increasing seawater temperature. Other elements of the ocean composition important to habitability, such as concentrations of CHNOPS elements used in biomass construction were assumed to be non-limiting and nutrients were not considered here as our goal is to calculate the instantaneous power available to life. The importance of nutrients is discussed in Section 5.

3.3 Methanogen parameter space

Methanogenic power supply calculations were performed using NutMEG (Higgins, 2021; Higgins & Cockell, 2020), which contains a 'typical optimal methanogen' class exhibiting typical behaviour of an exponentially growing hydrogenotrophic methanogen based on data from the literature. It has a cell volume of 3.44 μm^3 and a dry mass of 1 pg. The default number of moles of ATP produced per mole of CO_2 metabolised in the code is between 0.5 and 1.5 (Thauer et al., 1977; Nicholls & Ferguson, 2013), but for this study it was extended down to 0.25 and up to 2.0. This allows for effective energetic yields between 14 kJ (mol CO_2)$^{-1}$ and 130 kJ (mol CO_2)$^{-1}$(Supplemental Figure

S4), the lower limit approaching minimum free energies that methanogens subsist on in natural settings (Hoehler, 2004).

The rate constant of microbial methanogenesis has been constrained as a function of temperature by a comparison to the growth rates and CH_4 evolution rates of methanogens in empirical studies (Higgins & Cockell, 2020). This was independent of pressure, though the pressure range that was probed in the laboratory data was only 0.8–3 bar (Supplemental Figure S5). Uncertainty in the rate constant is taken in the decimal logarithm-space as ± 1 encompassing the majority of empirical methanogenic growth data. These rate constants were computed based on data from optimal energy and nutrient saturated conditions and hence present a conservative lower limit.

NutMEG was also used to calculate the power demand associated with the various temperatures in the parameter space, and does so using methods from the literature. We used three temperature-dependent power demands: i) derived directly from optimal growth of methanogens in the laboratory (Higgins & Cockell, 2020) ii) derived from the growth of anaerobic bacteria (Tijhuis et al., 1993) and iii) a theoretical minimum tied to the rate of amino acid racemization (Lever et al., 2015). The Higgins and Cockell (2020) power demand was calculated using NutMEG and the 'typical optimal methanogen' class so only requires temperature as an input. The Tijhuis et al. (1993) and Lever et al. (2015) power demands additionally require the dry mass of the organism and the energetic cost associated with protein synthesis respectively. The latter is computed internally in NutMEG (Higgins & Cockell, 2020) to between 790 and 2750 J (dry g)$^{-1}$ between temperatures of 273–400 K. This calculation is inclusive of amino acid synthesis and protein polymerization. We selected these three measures because it seemed appropriate to assume that the true maintenance cost experienced by putative microbes on Enceladus lies somewhere between these values. The racemization estimate acts as a fundamental thermodynamic minimum and the empirical estimates are based on the most favourable conditions and represent a maximum. Finally, to complement this analysis with an absolute minimum, we also examined whether power supplies on Enceladus can exceed the approximate minimum power supplies available to methanogens in Earth's marine subsurface (between 10^{-18} and 10^{-21} W cell^{-1} (Bradley et al., 2020)).

4 Results

4.1 Free energy availability

Figure 1 shows the nominal free energy of methanogenesis at various seawater temperatures and ocean pH values. As temperature increases, the free energy becomes less negative owing to a combination of the decreasing CO_2 activity (Supplemental Figure S2), increasing $\Delta G^\circ{}_M$ (Supplemental Figure S1) and the T contribution in equation 1 which offsets the decrease in $\ln Q$. More free energy is available at lower pH, which is also a result of higher CO_2 activity in less alkaline conditions. Figure 1 also shows how the pH is affected by increasing temperature from 273 K in the nominal case. High bulk ocean pH values may be decreased by over two units at 475 K, whereas pH values of 7, 8 and 9 decrease when warmed to ∼325 K, then invert and increase. Supplemental Figure S2 shows the pH values with increasing temperature, with the change in pH of pure water for comparison.

The Gibbs free energy of methanogenesis changes significantly within the chemical parameter space. The dotted contour lines in Figure 1 show how the free energy would be different in the best-case and worst-case scenarios for life offered by the parameter space. Here, the best-case scenario is a high salt ocean (maximising a_{CO2}) with maximised a_{H2} and minimised a_{CH4} and the worst-case scenario is a low salt ocean (minimising a_{CO2}) with minimised a_{H2} and maximised a_{CH4}. The endmembers

of the chemical speciation can have an equivalent effect to a shift by ± 0.5 bulk ocean pH units or ± 50 K in temperature. The CO_2 activity (dependent on the salt level via the mole ratio of carbonates/chloride determined by Postberg et al. (2009)) is the dominant contributor to this uncertainty as it also contributes to the determination of other key species' activities in the dissolved gas model that is adopted here (Waite et al., 2017). Supplemental Figure S6 shows some further contours, in the limiting case of each salt choice.

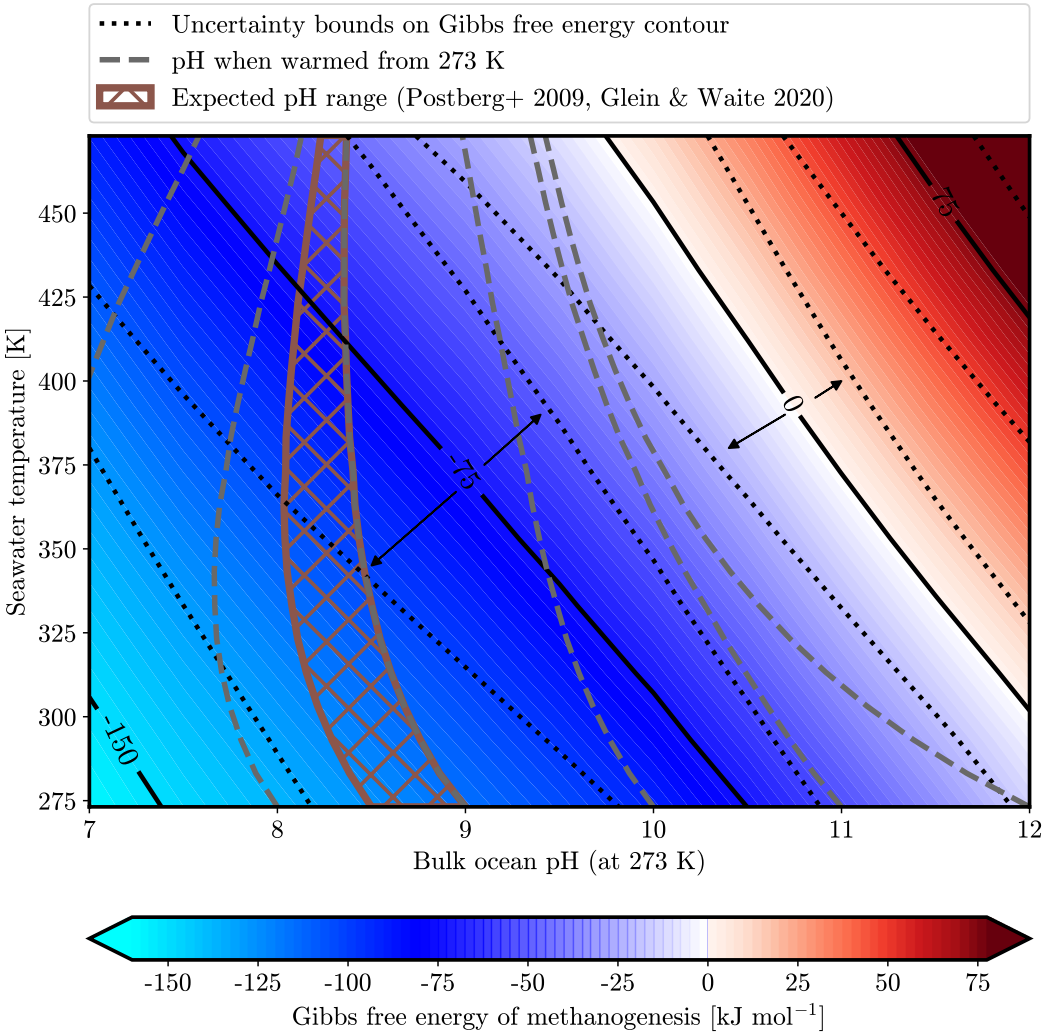

Figure 1. The Gibbs free energy of methanogenesis (equation 2) in seawater throughout the Enceladus ocean parameter space. Blue regions indicate those combinations of parameters where energy is available and red where it is not for a dissolved gas composition determined by the nominal salt case as described in the main text. The solid contour line also reflects this nominal free energy. The dotted contour lines show the total variation given by the chemical parameter space (salt endmember, a_{H2} and a_{CH4}) with respect to the closest solid line. The dashed lines reflect the nominal salt case pH variation with temperature.

The Gibbs free energy of ATP production also varies with temperature and similarly to methanogenesis it is dominated by the T term in equation 1 at low temperatures, but these changes are minor in comparison to variation in n_{ATP} (Supplemental Figure S4). At $T > 400$ K, the Gibbs free energy yield per mole of ATP begins to decrease owing to contributions from $\Delta G^{\circ}{}_{\mathrm{ATP}}$ (Supplemental Figures S1 and S4). As the internal composition of the methanogens considered was fixed, ΔG_{ATP} does not vary with environmental pH here. This is not strictly representative of all thermoalkaliphiles on Earth, whose adaptations vary between maintaining a trans-membrane pH gradient (i.e. changing internal pH with external pH) to maintaining their internal pH when faced with varying environmental pH stresses (Mesbah et al., 2009). As our ΔG_{ATP} does not vary with environmental pH, it yields an energetically similar effect to preserving the trans-membrane pH gradient (a consistent proton-motive force).

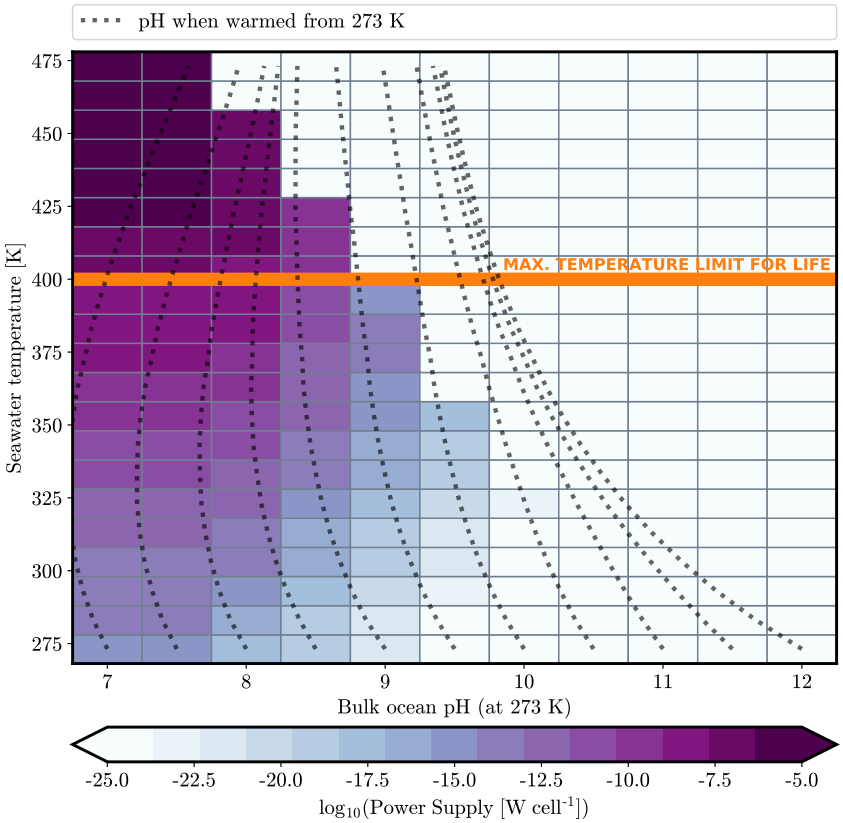

Figure 2. Power supply available to a hydrogenotrophic methanogen in the nominal case of the parameter space at various seawater temperatures and bulk ocean pH values. The nominal case refers to an ATP yield per mole CO_2 of 1.0, NutMEG default methanogenesis rate constant, and a dissolved gas composition determined by the nominal salt case as described in the main text. Also noted at 400 K is an approximate maximum temperature limit for life and dotted lines reflect the nominal salt case pH variation with seawater temperature.

4.2 Net power supply

The power supply available to an organism is determined by both its microbial machinery and the free energy available from the environment. The nominal instantaneous power supply for a typical methanogen was calculated at intervals of seawater temperature and a bulk ocean pH value of 10 K and 0.5 units respectively and is shown in Figure 2. This uses the ΔG_{M} plotted in Figure 1, an n_{ATP} of 1 mole per mole of CO_2 and the nominal rate constant of methanogenesis at the selected temperature. Figure 3 shows endmember values of this power supply given by the parameter space when $n_{\mathrm{ATP}} = 1$ and other variables in Table 1 are either minimised or maximised. Also noted on Figures 2 and 3 is a maximum temperature limit for life at approximately 400 K. This reflects the highest temperatures observed for survival and growth of life on Earth, though it has been hypothesised that a true upper limit may be as high as ∼425 K (Cowan, 2004). It is possible that this limit at 400 K could also decrease with increasing pH, as thermoalkaliphiles appear to be rare on Earth (Harrison et al., 2013). This could be explained by the difficulty in accessing Earth's scarce quantity of high-pH high-temperature environments, or signal that the combined extremes of temperature and high pH are particularly difficult to overcome (for example by promoting the cleavage of biomolecules (Hoehler, 2007)).

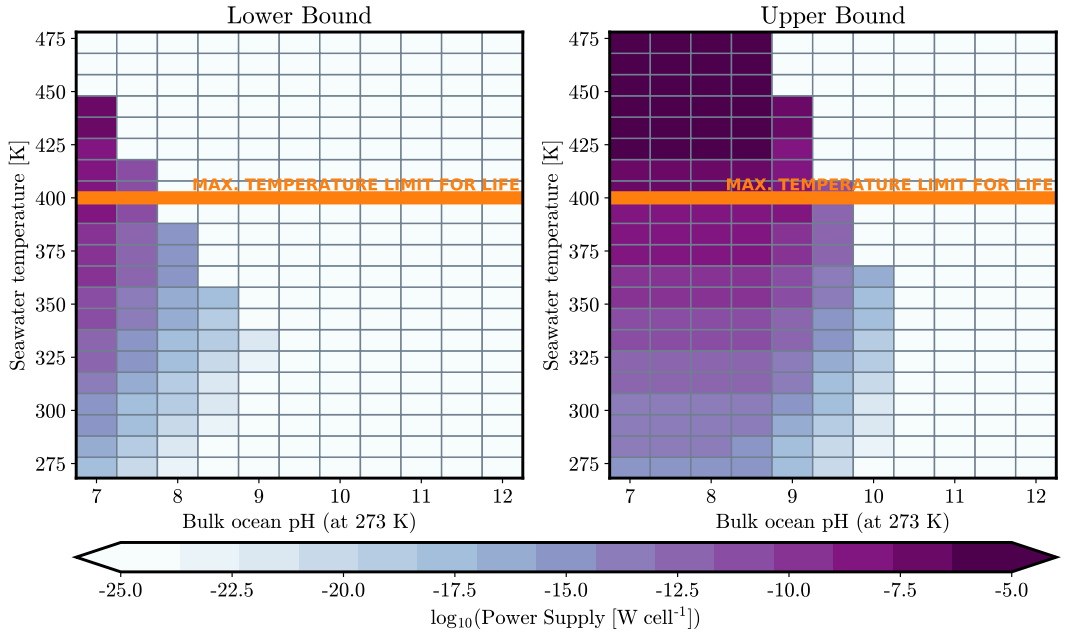

Figure 3. Power supply available to a methanogen at the limiting cases of the parameter space at various seawater temperatures and bulk ocean pH values. Left: low salt endmember, minimised a_{H2} and k, maximised a_{CH4}. Right: high salt endmember, maximised a_{H2} and k, minimised a_{CH4}. Both at $n_{\mathrm{ATP}} = 1.0$, limiting cases of n_{ATP} are shown in Supplemental Figure S7 and S8.

The amount of ATP that a methanogen attempts to produce per mole of CO_2 defines a minimum amount of available Gibbs free energy for the metabolism to run efficiently. This means that while a larger n_{ATP} allows for more efficient energy extraction when ΔG_M is highly negative, it relies on high energy yields being available in perpetuity. Similarly, a low n_{ATP} allows for a methanogenesis-driven power supply to low energy yields, but is less versatile to extract more power in higher energy environments. This is demonstrated in Supplemental Figures S7 and S8 which present variants of Figure 3 with different n_{ATP} values.

4.3 Variance in power supply from the parameter space

The endmembers of power supply presented above give some insight into how wide ranging these values could be in the ocean's parameter space. To elucidate how each parameter contributes to this variation, samples were taken across their possible values (Table 1). Figure 4 shows the total variance for a random uniform sampling of n_{ATP}, k, a_{H2} and a_{CH4} across bulk ocean pH values of 8, 9, 10, and in the nominal and limiting cases of ocean salt content. Each plot contains a sample of 2000 cases. In general, the variance caused by this parameter space is approximately (+2)–(−3) orders of magnitude regardless of temperature or pH choice. In some limiting cases, such as the top-left and center-left plots of Figure 4, the bounds of variance decrease. This is because the NutMEG model prevents the simulated methanogens from consuming CO_2 at a faster rate than has been observed in its input database (Higgins & Cockell, 2020). The upper bounds in the center-left plot approach this maximum metabolic rate with increasing T. In the top-left plot, the nominal case is already above the maximum metabolic rate and many combinations of the parameter space are restricted to a smaller variance.

In some cases, the expanded parameter combination can provide power when the nominal case cannot. These are characterised in Figure 4 by red bins. The key driver of this is low n_{ATP} values decreasing the free energy requirement for microbial methanogenesis to operate, as discussed above.

Table 2. Variance contribution of the parameter space to the methanogenic power supply in $\log_{10}$ space. These contributions are independent of bulk ocean pH, seawater temperature, and ocean salt content. Plots of the complete contributions for 20 combinations of pH_{bo} and T are available in the Supplemental Dataset.

Parameter	**Best-case variation for life**	**Worst-case variation for life**
a_{CH4}	+ 0.1	− 0.1
a_{H2}	+ 1	− 2
n_{ATP}	+ 0.5	− 0.5
k	+ 1	- 1

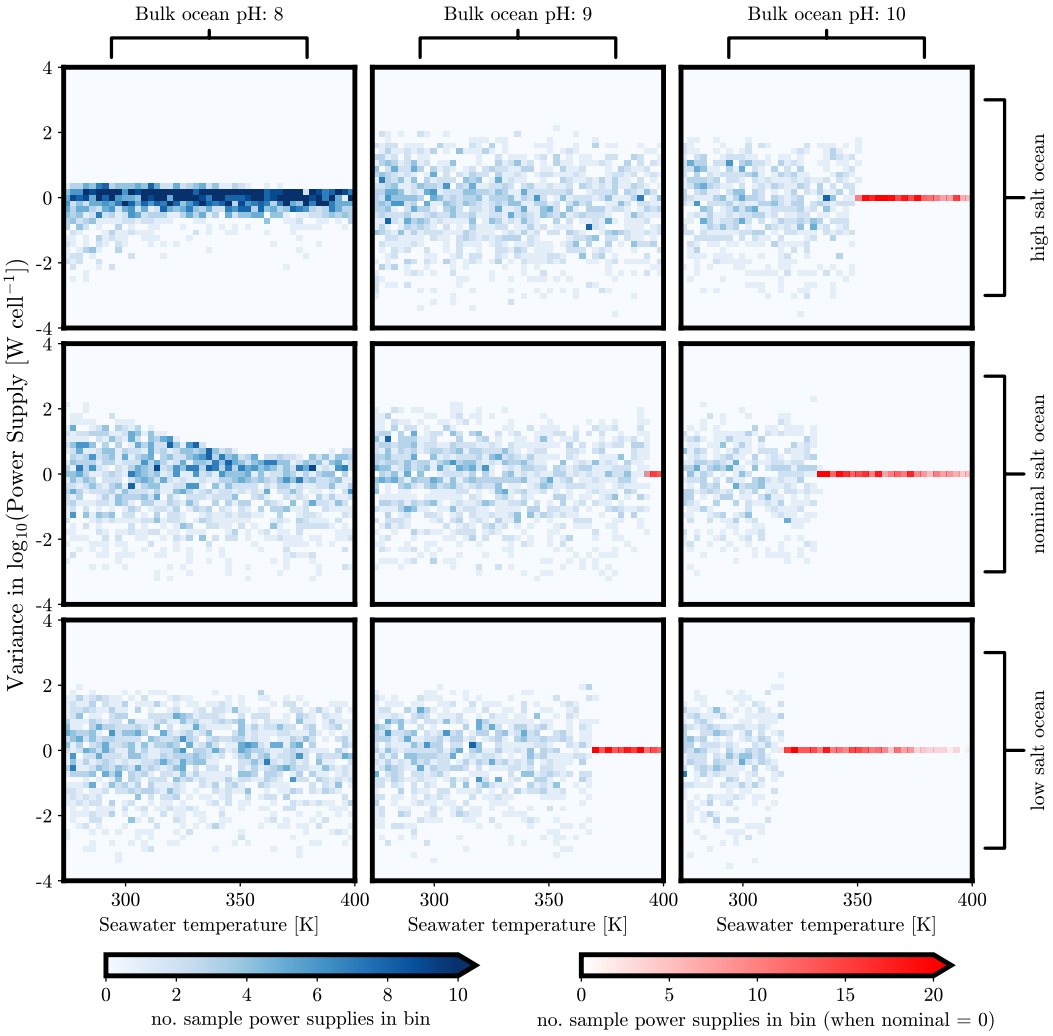

Figure 4. Total variance within the parameter space from the nominal power supply at various combinations of seawater temperature, bulk ocean pH and level of salt in $\log_{10}$ space. Parameter spaces within these plots are between endmembers of a_{CH4}, a_{H2}, n_{ATP} and k and T range 273–400 K. The nominal case refers to an ATP yield per mole CO_2 of 1.0, NutMEG default methanogenesis rate constant, and a composition determined by the nominal salt case as described in the main text, plotted in Figure 2. Samples were taken from a flat distribution in each parameter. Sample size was 2000 per plot. The individual contribution of each of these is summarised in Table 2 and in the Supplemental Data. The blue shades show the total variance from the nominal power supply in $\log_{10}$ space and the red shades show areas where the wider parameter space provided power supplies when the nominal case could not.

The contributions of the individual parameters to this variance were explored and are summarised in Table 2. Random uniform samples were drawn between the endmembers of $\log_{10}(k)$, n_{ATP}, a_{H2} and a_{CH4} (Table 1) with all other parameters taken at their nominal values. As with the overall variance, there is no variation with temperature, pH choice or salt level unless the maximum metabolic rate is approached. This maximum metabolic rate represents the apparent limit of Earth methanogens so could potentially be exceeded by hypothetical Enceladus methanogens. The largest contribution is from a_{H2}, due to the large range of values of volume mixing ratio and its conversion to the concentration of dissolved H_2 exacerbating its uncertainty, and the rate of metabolism being dependent on $(a_{\mathrm{H2}})^4$, along with contributions of its effect on the available Gibbs free energy of reaction via the reaction quotient (Equation 1). In contrast, the contribution of a_{CH4} is much smaller as it is not a variable in the rate calculations, only the Gibbs free energy. The variance contribution of k is uniformly distributed between ± 1 order of magnitude, reflecting its contribution to the microbial kinetics (Supplemental Figure S5; Higgins and Cockell (2020)). The variance contribution of n_{ATP} is minor in comparison to k and a_{H2}, but as discussed above the choice of n_{ATP} can extend the availability of power supplies to higher temperatures and higher bulk ocean pH values. These contributions are plotted at various temperatures, pH and salt concentration values in the Supplemental Dataset.

4.4 Energetic habitability of the parameter space

To be habitable, an environment must provide enough power to meet the demands of survival imposed by its physico-chemical settings. The power supplies computed from the parameter space were compared against characteristic power demands in various metabolic states from the literature, corrected for the size of the methanogen. The latter powers are shown by the solid bars in Figure 5. The Higgins and Cockell (2020) 'maintenance' powers are derived from methanogenic growth data in optimal conditions; the Tijhuis et al. (1993) maintenance powers are from a more general case for anaerobic bacteria; the Lever et al. (2015) maintenance powers characterise the cost of protein repair whereby proteins are replaced after between 2% and 10% of their constituent amino acids are racemized; and the Bradley et al. (2020) power range is the approximate minimum power supply available to (and possibly survived by) methanogens in Earth's subseafloor sediments. The three maintenance power models are temperature dependent and do not account for the environmental pH, hence the horizontal bars on the left hand side of Figure 5. As pH deviates from neutrality, it is expected that the power demand will increase (Hoehler, 2007). Similarly, the minimum power supplies are shown as a horizontal bar on the right hand side of Figure 5. This range represents Earth's subseafloor sediments, and were calculated at $T = 278$ K and $P = 100$ bar (Bradley et al., 2020) so a true minimum is likely to be higher than this at elevated temperatures.

The characteristic power supplies in Figure 5 are the nominal values at 275 K, 300 K and 325 K changing with bulk ocean pH on the left and at bulk ocean pH 8, 9, and 10 changing with seawater temperature on the right (solid lines), alongside high salt and low salt nominal values (dashed lines), and the best-case and worst-case scenarios offered by the parameter space (dotted lines). From this figure it is clear that some configurations of the parameter space offer power supplies which exceed the various power demands in the literature and some do not — typically those at higher bulk ocean pH and lower seawater temperature. The configurations that meet the thresholds of the four habitability measures are shown in Figure 6 for $n_{\mathrm{ATP}} = 1$. The lighter shaded segments can be exceeded by more of the parameter space than the darker shaded segments, which are only 'habitable' to the cases with higher power supply yields. Much of the parameter space with a bulk ocean pH of less than 10 exceeds the expected minimum power supply available to methanogens on Earth, taken as a conservative 10^{-18} W/cell, the upper limit of such predictions (Bradley et al., 2020).

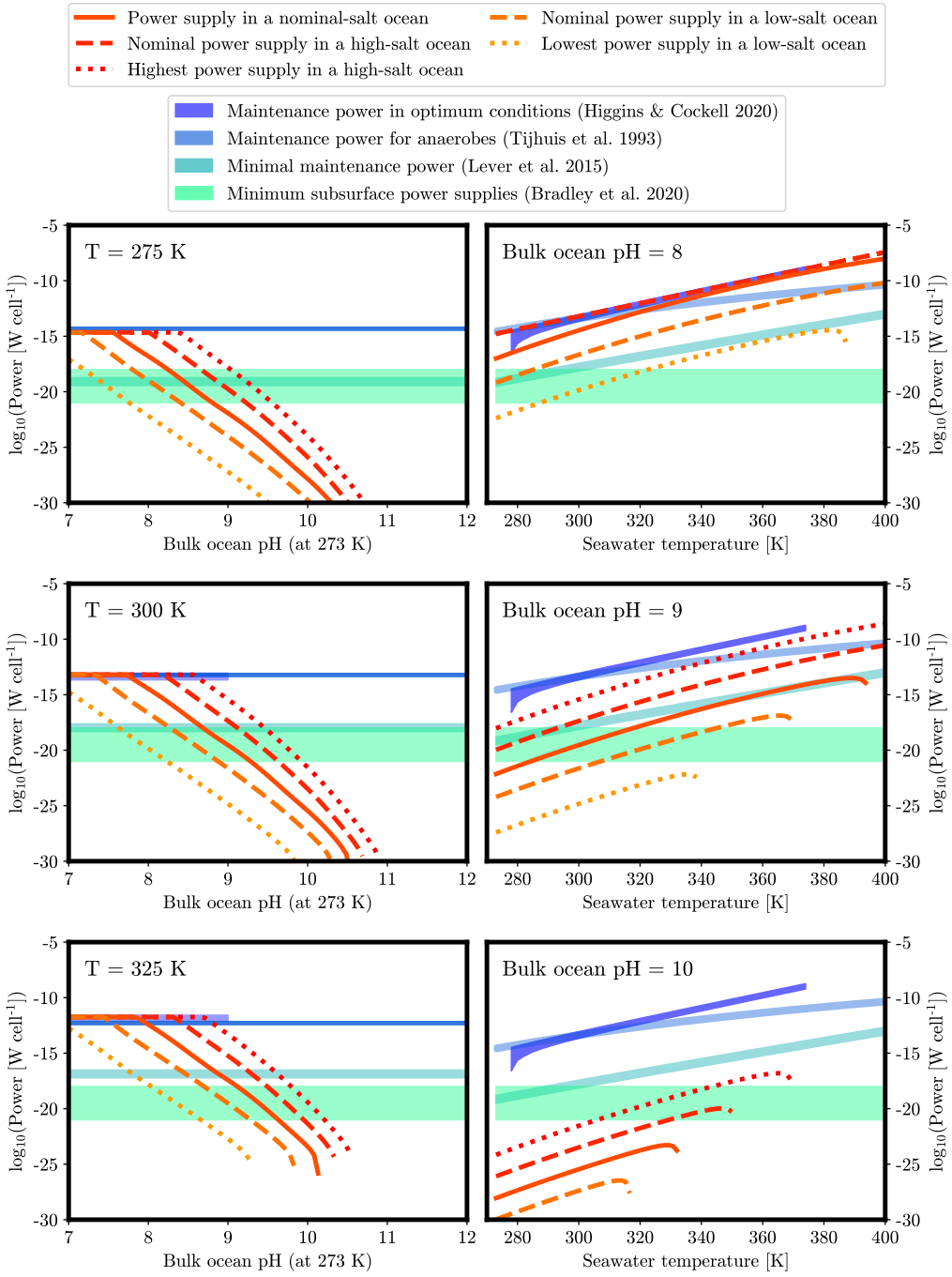

Figure 5. Power supply available in select bulk ocean pH and seawater temperature T combinations, with representative estimates of power demands due to temperature in those settings. The left hand column is at fixed T and changing bulk ocean pH, the right hand column is at fixed bulk ocean pH and changing T. Power supplies plotted are the nominal case (solid line), nominal high- and low salt cases (dashed lines) and the endmembers that the composition may allow in those cases (dotted lines). The colored bars represent the power demands expected in the given conditions. The Higgins and Cockell (2020) bar only partially covers temperature and bulk ocean pH values as these were the limits of the data input to their model. This figure is for $n_{\mathrm{ATP}} = 1.0$, identical graphs for $n_{\mathrm{ATP}} = 0.25$ and $n_{\mathrm{ATP}} = 2.0$ are available in Supplemental Figure S9 and S10 respectively.

Similarly, there could be a large enough instantaneous power supply to exceed minimal maintenance estimates (Lever et al., 2015) at bulk ocean pH values of less than 9.5.

Some cases of the parameter space suggest that the chemical disequilibrium may be large enough to host optimal methanogenic growth (Figure 6, top row), similar to that observed in laboratory experiments. However, this would only be the case if the ocean has a pH of 8.5 or less and the ocean has a high salt content. Variation in n_{ATP} cannot increase this to higher pH values (cases for $n_{\mathrm{ATP}} = 0.25$ and $n_{\mathrm{ATP}} = 2.0$ are shown in Supplemental Figures S11 and S12). Because we do not consider hydrothermal fluid as a contributor to the chemical composition, at elevated temperatures we present a conservative bioenergetic scenario. As such, that even some of the seawater parameter space can host optimal methanogen growth brings tantalising possibilities for the habitability of putative hydrothermal systems with higher activities of methanogenesis ingredients, particularly H_2. Alternatively, highly alkaline hydrothermal fluids could shift the carbonate speciation and decrease a_{CO2} compared to seawater. Abiotic reactions and/or microbial competition could also create significantly different conditions in these systems. Some of these possibilities are explored in Sections 5.2 and 5.3 but to confidently quantify these effects requires more information on the nature of Enceladus' hydrothermal fluids.

5 Discussion

Despite the optimism about the habitability of icy moons, and particularly Saturn's moon Enceladus, we still do not have sufficiently precise observational constraints on the parameters necessary to assess the habitability of such environments in the context of the currently known limits to life. In this work, we have sought to address this by quantifying the energy and power available to hydrogenotrophic methanogens under a range of possible parameter values in the Enceladus bulk ocean to both identify what factors might determine the habitability of the seawater and illuminate which parameters might be a priority for improved measurements in future missions.

5.1 Implications for Enceladus' habitability

Observations of Enceladus in recent decades have revealed tantalising details of its subsurface ocean, allowing it to be resolved in unprecedented detail in comparison to other icy moons. Still, the breadth of parameter spaces that the Enceladus ocean may possess is significantly larger than one might expect. We have stripped back models of the icy moon's subsurface to focus on its ocean — considering Enceladus seawater at both cold and elevated temperatures — as derived from Cassini's measurements in an attempt to find out where in its observable parameter space conditions would permit the persistence of Earth-like methanogens. This has allowed us to identify the most important drivers of habitability for methanogens in our model as being the pH and salt/carbonate content, because they are linked to the activities of H_2 and CO_2.

Our results show that both energetically habitable and uninhabitable environments within the possible parameter space of Enceladus' subsurface ocean may exist and we have been able to quantify where the energetic thresholds for habitability may lie for methanogens. To provide useful energy to methanogens, a 273 K ocean that is relatively high in salts and carbonates must have a pH $\leq$10. If the ocean has a relatively low concentration of salts and carbonates, the pH needs to be 8 or lower to meet the minimum power supplies required by methanogens on Earth, with this value increasing to pH 9 or lower at temperatures above 360 K. We stress that these are only energetic thresholds for habitability which do not consider other important measures such as nutrient content and the potential for increased energy availability in hydrothermal fluid (see below). As such, these results should be considered conser-

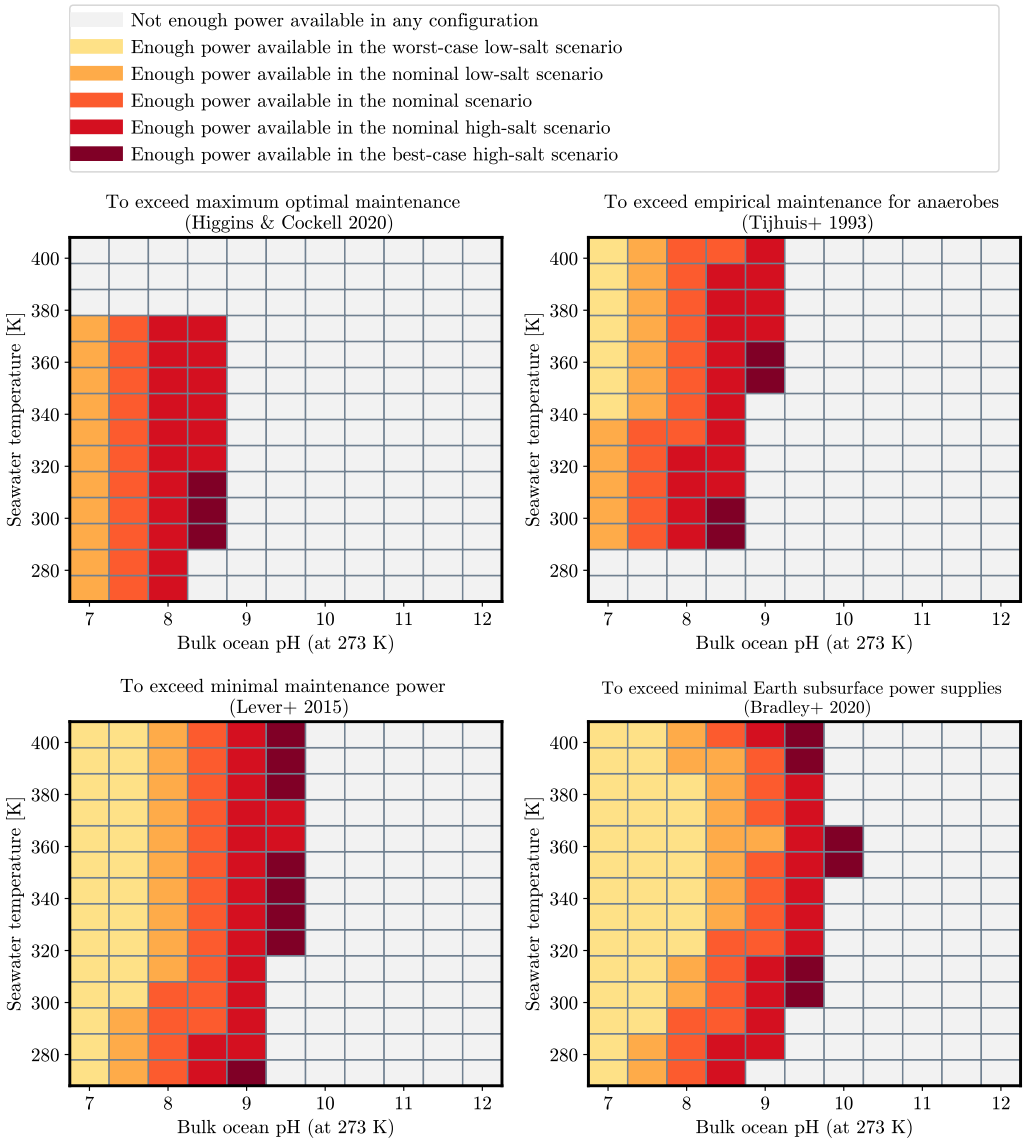

Figure 6. Areas of the Enceladus ocean parameter space which meet various criteria for habitability. Segments are filled when part of the parameter space's predicted power supply exceeds the power demand posed by one of four scenarios: top-left) exponential growth of methanogens; top-right) exponential growth of anaerobes; bottom-left) cost of protein repair after amino acid racemization; bottom-right) minimal power supplies to methanogens in Earth's deep marine subsurface. These cases are for $n_{\mathrm{ATP}} = 1.0$, companion graphs for $n_{\mathrm{ATP}} = 0.25$ and $n_{\mathrm{ATP}} = 2.0$ are available in Supplemental Figures S11 and S12 respectively.

vatively optimistic when suggesting low temperature habitable regions, and somewhat pessimistic when higher temperatures and pH values appear uninhabitable.

For highly efficient metabolisms, some regions of the parameter space may be able to meet the maintenance requirements of exponential growth, for example in a high salt case at pH 8.5 or lower, and in a low salt case at pH 7. Because exponential growth would not be sustainable for geological timescales, if future observations determined that such conditions existed in perpetuity on Enceladus with no further evidence of life they could be interpreted as an uninhabited (or vacant) habitat (Cockell, 2011). Alternatively, if such conditions were fleeting and Enceladus inhabited, methanogens in non-growing states could be poised to take advantage of the short-lived energy availability as life does in low-energy environments on Earth (Bergkessel et al., 2016). One interesting example of this could be variability in Enceladus' geological activity owing to irregular tidal heat generation or transport processes (O'Neill & Nimmo, 2010) causing 'waves' of energy for life. Another more speculative idea could be that if Enceladus is young (∼100 Myr) (Ćuk et al., 2016) and life was only recently established, it may not have yet reached a steady state with the environment. In any case, if Enceladus is ∼100 Myr old, material exchange with the inner solar system is a low probability event and so it would be likely that, if inhabited, such life would have emerged independently from Earth (Cable et al., 2020). As we do not know the probability of life emerging on Enceladus, a vacant habitat or uncertainties in our model could yet be the simplest explanations.

5.2 Uncertainties in composition owing to hydrothermal activity

A remaining question is the influence of hydrothermal activity on the oceanic composition at elevated temperatures. The chemical makeup of these warmer regions on Enceladus is likely to be significantly affected by interactions at the rock-water boundary, including a_{H2}, a_{CO2}, a_{CH4} and nutrient content. If Enceladus' hydrothermal systems are similar to those on Earth, we would expect significant chemical differences compared to the ocean above. This includes the potential for different activities of methanogenesis ingredients, particularly increased a_{H2} and possibly a_{CO2}. This could yield higher instantaneous power supplies for life, perhaps such that systems with lower salt content and/or higher pH could appear more habitable than our results suggest. Alternatively, the system could become depleted of one or more key energy/nutrient sources for methanogens from abiotic reactions or competition, discussed below. Furthermore, the discharge of these species from the plume will generate a chemical gradient in the ocean which could affect their abundances throughout it, even at low temperatures. Including such influences could provide more habitable niches with H_2 and CO_2 concentrations exceeding the ones used here, but would vastly complexify the parameter space as presented in this work. Future work which explores the scope of hydrothermal activity on Enceladus coupled with the models we have developed here would be valuable for more conclusively assessing its habitability in these critical regions.

Our results above 273 K could still be useful for some environments which may exist on Enceladus. One example could be seawater in an aquifer with minimal localised hydrothermal activity. On Earth, cool basaltic ridge-flank hydrothermal systems (≤293 K) have very similar compositions to seawater at the ocean floor (Wheat et al., 2017). Similar settings could exist on Enceladus in water-rock systems which are already close to non-redox equilibrium aside from a small change in temperature. The composition would be most seawater-like in a significantly carbonated sub-seafloor layer which could be present in a heterogeneous structure of Enceladus' rocky core (Glein & Waite, 2020). At temperatures of tens of degrees Celsius, element exchange between water and rock could also be kinetically inhibited if the residence times of the aquifer fluids are sufficiently short. Seawater could seep into these systems and

be gently warmed along the conductive geothermal gradient, with composition and habitability similar to that of our heated seawater.

Our results can also approximate the heated seawater contribution to relatively low-temperature mixed fluids near hydrothermal systems on Enceladus. The composition of these tentative habitable zones would be determined from both that of the heated seawater and hydrothermal fluid. On the one hand, if the water-rock temperature is very high ($\gg$400 K), then mixtures at temperatures well into our parameter space could be dominated by seawater. On the other hand, if the water-rock temperature is much lower, then most elevated temperatures of our parameter space will be dominated by the hydrothermal contribution. Ultimately, we need to know the temperature of the hydrothermal systems and degree of mixing with seawater to determine the extent to which our results at elevated temperatures may contribute to mixed hydrothermal fluids on Enceladus. The scale and nature of water-rock interaction on Enceladus remains an open question, but our heated seawater approximation can act as a starting point for the chemical composition and habitability of systems which are dominated by seawater.

5.3 Other limitations of the parameter space and model

This study necessarily involved other simplifications and assumptions and here we elaborate what these are. One limitation is in the establishment of a sufficient power supply for habitability. Both the rate of microbial energy uptake and maintenance powers are difficult to determine empirically. The maintenance power of organisms can vary significantly depending on environmental conditions and their growth state (e.g. between lag, growth and stationary phases) (Hoehler & Jørgensen, 2013). Four characteristic maintenance powers were used here, covering the minimum energy fluxes available to methanogens in Earth's subsurface, up to the expected cost when exponentially growing in the laboratory. Three of these maintenance power models use temperature as their defining variable but none of them account for the effects of pH. It is expected that maintenance power increases as the pH deviates from neutrality, but while energetic costs at different pH values can be estimated, to our knowledge no empirical quantification has been published yet (Hoehler, 2007).

Limitations in the datasets for these maintenance power models should also be highlighted. The Higgins and Cockell (2020) dataset covers optimal methanogen growth between 288–371 K and pH values of 6–9.1. The Tijhuis et al. (1993) dataset covers microbial growth temperatures between 280 and 330 K. As their results were resolved to an expression in T, we tentatively extended them to 400 K for our analysis. Better constraints on the power demands owing to various physico-chemical parameters including temperature, pH, pressure, salinity etc. are needed to further improve our assertions of (unin)habitability.

Beyond the local energetic availability, the choice of n_{ATP} highlights the efficiency of the microbial machinery towards the rate of energy uptake. While a low n_{ATP} allows energy extraction at low energetic availability, this hinders the power supply when there is more energy available per mole of CO_2. Similarly, a high n_{ATP} allows a large fraction of the available free energy to be extracted when it is plentiful, but makes the metabolism thermodynamically unfavorable in periods of low energy availability. If versatility in the number of ATPs produced per mole of CO_2 with a changing environment were introduced to the model, the methanogens would be able to 'adapt' to their settings allowing for different behaviour in low-energy and high-energy environments as described above. Similarly, alternative sources of energy to ATP could be considered such as pyrophosphate, acetyl phosphate or thioesters. This would lead to an alternative amount of Gibbs free energy conserved by the organism (in this work, ΔG_{ATP}). We would expect similar results to this work, provided such alternative

Gibbs free energies fell within the broad scope considered here (Supplemental Figure S4). Furthermore, as we have shown in this work, the changes in energy availability often come with significant changes in temperature and pH, variation toward which organisms typically have a low tolerance.

Our results can be compared to the limits of methanogens on Earth. Methanogen species are known that grow optimally at salinities of up to 9–12 % (Oren, 2011), and many can tolerate salinities higher than this (Kulp et al., 2007; McGenity, 2010). The highest salinities from this work (pH 12 in the high salt case) are ≈4 % so the salinity of the ocean from our model should fall well within these limits. However recent modelling studies suggest the salinity could be significantly higher deeper in the ocean (Lobo et al., 2021). Methanogens have not yet been observed to grow at pH values higher than ≈10 (Taubner et al., 2015), but their presence has been indicated at locations such as Lost City which contains fluids at higher pH than this (Brazelton et al., 2006), so methanogenesis above pH 10 should not be ruled out. Our results indicate that methanogenesis becomes severely energetically limited when the Enceladus bulk ocean pH approaches these values, so survival would require extra adaptation such as CO_2 concentrating mechanisms. However, there are significant chemical differences such as increased H_2 activity that could be expected between hydrothermal fluid and our heated seawater model, as discussed above. In alkaline settings on Earth, methanogens are typically outcompeted for H_2 by sulfate reducers (McGenity, 2010). Ray et al. (2021) computed that the dissolved ${SO_4}^{2-}$ concentration could be up to ∼1 mmol $(\mathrm{kg\ H_2O})^{-1}$ so such competition on Enceladus is worth consideration. In a mixed fluid, abiotic reactions between H_2 and ${SO_4}^{2-}$ could deplete these species limiting their availability for both methanogens and sulfate reducers, but such reactions are thought to be kinetically inhibited at Enceladus' expected alkaline pH (Tan et al., 2021). Even so, the possibility of abiotic H_2 sinks at high temperatures should not be ruled out; such processes are common in hydrothermal systems on Earth (e.g. McDermott et al., 2020; Worman et al., 2020).

Further to the points above, hydrogenotrophic methanogenesis may not be the only metabolism that Enceladus' subsurface ocean can host. While CO_2 is the most biologically useful oxidant directly observed (Hand et al., 2020), mechanisms of delivery for other oxidants such as O_2 and H_2O_2 have been proposed which allow for a variety of possible metabolisms to be considered (Ray et al., 2021). Still, despite these alternatives methanogenesis appears to have the highest energy yield and biomass potential for a weakly-alkaline ocean owing to large dissolved CO_2 and H_2 activities in comparison to other biologically useful chemical species (Ray et al., 2021). Enceladus' surface radiation flux is much less than that of Europa, making radiolytic processing of the surface ice provide a smaller input of oxidants. This may restrict Enceladus' inventory of biologically available oxidants (Paranicas et al., 2012; Hand et al., 2020); alternative sources could include radioactive decay within the ocean or in the deeper interior (Ray et al., 2021; Bouquet et al., 2017).

Nutrient availability is another cornerstone of an environment's habitability. Enceladus' nutrient inventory is not yet completely known and neither iron, phosphorus nor sulfur — key elements required by life on Earth — have been confidently detected, only modelled (Lingam & Loeb, 2018; Cockell et al., 2021; Ray et al., 2021; Magee & Waite, 2017), but they are widely expected to be present. While a detection of H_2S has been reported (Waite et al., 2009), subsequent analyses suggest ambiguity in its identification (Magee & Waite, 2017). A possible nitrogen source for life is available in the form of ammonia (Waite et al., 2017; H. T. Smith et al., 2008), or ammonium if the ocean pH is below ∼10. Carbon sources other than CO_2 and CH_4 have also been reported in the form of diverse types of organic compounds that span a spectrum from simple to complex (Waite et al., 2009; Postberg et al., 2018; Khawaja et al., 2019). While the results presented here identify some power supplies

which can overcome maintenance costs, nutrients such as these are required not only for synthesising new biomass, but also for cell repair (Hoehler, 2007). This means that our results indicating habitability are optimistically conservative. A low availability or lack of any of these unconstrained nutrients will foster more challenging conditions for any form of life, restricting the ease at which it can survive, grow and evolve (Higgins & Cockell, 2020). Consequently, the parameter space could be less habitable than we have presented it here.

This study focused on the instantaneous habitability of the ocean using the chemical disequilibrium indicated by geochemical modelling and Cassini observations. To be habitable on longer timescales requires substrate and nutrient resupply. Rates of serpentinization and other rock alteration processes have been proposed (Steel et al., 2017; Waite et al., 2017; Taubner et al., 2018; Zandanel et al., 2021; Cable et al., 2020; Glein & Waite, 2020) as a way to supply further CO_2 and H_2 on geological timescales, but these predictions vary over several orders of magnitude. Methane may be continuously removed from the ocean by plume outgassing activity. In order to confidently estimate the sustainable levels of biomass in the habitable regions of this parameter space, more information on the nutrient content of the ocean is needed, along with the rate of supply of such nutrients and the methanogenesis reactants (Cable et al., 2020).

Finally, as a natural system, Enceladus' ocean is not homogeneous, and there cannot be a one-size-fits-all equation for its composition in any given place. While we attempted to span as wide a possible parameter space as practical for this study, a conclusion that oases of habitable niches exist (such as Figures 2–6 at pH 7–8.5) cannot be confirmed until the exact nature of the ocean is resolved further. On the other hand, conditions on Enceladus not included in this parameter space such as more complex hydrothermal systems in the rocky core or a possible highly saline deep-ocean could well provide far more diverse and lucrative redox energy sources.

5.4 Recommendations for future work and missions

Our results complement recent studies which aim to elucidate whether Enceladus could — or has ever been — habitable or inhabited using an array of innovative techniques (e.g. Waite et al., 2017; Steel et al., 2017; Ray et al., 2021; Affholder et al., 2021). It is encouraging that such analyses rarely suggest that Enceladus is completely uninhabitable, but each model (including our own) has unique limitations. By continuing to explore icy moon habitability and determine detectable biosignatures using new techniques we can inform future missions on the critical variables to measure when they next visit (MacKenzie et al., 2021; Cable et al., 2021).

This work also highlights some key goals to pursue by either modelling analyses, laboratory experiments or future observations to further constrain the habitability of Enceladus' ocean, including:

1. **Determine whether the ocean composition can be directly quantified from the salty plume ice composition**. For instance, can the extent of fractionation and/or concentration processes between leaving the ocean and entering the plume be determined for each species? This would allow us to better constrain the geochemistry of the ocean.
2. **Further our understanding of the relationship between the dissolved H_2 concentration and the measured H_2 mixing ratio in the plume**. This may be complicated from the present model by different outgassing rates of H_2 and CO_2, as well as heterogeneity with ocean depth (Glein et al., 2018; Waite et al., 2017).
3. **More tightly constrain the ocean pH and temperature** at its floor. This could be accomplished using geochemical indicator species/ratios in the plume,

or via direct measurement of pH in a melted sample of collected plume ice grains or plume "snowfall" on the surface.

4. **Improve the precision of the concentration of carbonates in the ocean**, which will be supported by point 1) above. Further analysis of Cassini CDA data may provide new insights. Future measurements of anions in plume ice grains (Cassini CDA could only detect cations), or other approaches to determine carbonate alkalinity would enable a significant advancement.
5. **Add more concrete constraints to the Enceladus ocean's possible nutrient inventory**. Ideally this would come from direct measurements of species that contain sulfur or phosphorus. Alternatively this could be achieved indirectly from observations or experimental work that better constrain geochemical processes that deliver these elements to the ocean (Cable et al., 2020).
6. **Improve our understanding and inventory of thermoalkaliphiles on Earth** and how they might fare in Enceladus-like conditions. At present, there are no perfect analog environments of Enceladus' ocean as we understand it (Glein et al., 2018). Culture experiments which are representative of the ocean's geochemistry as predicted by models such as ours would help determine whether these conditions can be habitable for known life.
7. **Constrain the nature of Enceladus' hydrothermal systems**. These are arguably some of the most promising known potentially habitable zones beyond Earth. Confidence in their physico-chemical nature, including for instance their composition, temperature and interactions with seawater is tantamount to deducing whether they are habitable or not.

Continuing avenues of research such as these will not only elucidate more information on the Enceladus ocean, but will further its applicability as a stepping stone for studies of other extraterrestrial liquid water environments, such as those on Mars, Ceres, Europa, Ganymede, Titan, and possibly Pluto and Triton.

6 Summary

We have used coupled geochemical and microbial metabolic models (The Geochemist's Workbench and NutMEG) to explore the possible physical and chemical parameter space of the Enceladus ocean to identify where thresholds between habitable and uninhabitable conditions could lie for hydrogenotrophic methanogens. Our results emphasise the importance of pH and the concentration of carbonates in determining these thresholds with current models — with implications for mission measurement priorities — and they show how, with respect to this metabolism, a non-homogeneous Enceladus could possess pockets of habitability. This work has also shown how microbial metabolic models can be used to explore the diverse physical and chemical combinations in extraterrestrial environments to 'map' their habitable and uninhabitable spaces. Beyond the example of Enceladus, similar approaches can be applied to other astrobiology targets in the solar system, for example on jovian moons using results from the Europa Clipper and JUICE missions.

Data Availability

The source code for NutMEG and links to its documentation are available in the NutMEG github repository: `https://github.com/pmhiggins/NutMEG`, and archived in Zenodo (Higgins, 2021). For this work, version 1.0.0 was used (doi: 10.5281/zenodo.4746807). All of the code required to replicate these results, as well as data files containing the data plotted in all figures are available in the NutMEG-Implementations GitHub repository, in the Enceladus2021_ParameterSpace directory: `https://github.com/pmhiggins/NutMEG-Implementations` (also archived in Zenodo, doi: 10.5281/zenodo.4746637). Supplementary datasets are available on figshare (doi: 10.6084/m9.figshare.14562144)

and summarised in the Supporting Information document. Supplementary Text, Tables and Figures are available in the Supporting Information document.

Acknowledgments

This work was supported through the Science and Technology Facilities Council (STFC) grant ST/R000875/1 and an STFC studentship to PMH. CRG acknowledges support from NASA through the astrobiology project Habitability of Hydrocarbon Worlds: Titan and Beyond. We thank two anonymous reviewers for their detailed and constructive comments.

References

Affholder, A., Guyot, F., Sauterey, B., Ferrière, R., & Mazevet, S. (2021). Bayesian analysis of Enceladus's plume data to assess methanogenesis. *Nature Astronomy*, 1–10. doi: 10.1038/s41550-021-01372-6

Albe, K. R., Butler, M. H., & Wright, B. E. (1990). Cellular concentrations of enzymes and their substrates. *Journal of theoretical biology*, *143*(2), 163–195. doi: 10.1016/S0022-5193(05)80266-8

Bergkessel, M., Basta, D. W., & Newman, D. K. (2016). The physiology of growth arrest: uniting molecular and environmental microbiology. *Nature Reviews Microbiology*, *14*(9), 549–562. doi: 10.1038/nrmicro.2016.107

Bethke, C. (2008). *Geochemical and biogeochemical reaction modeling* (2nd ed.). Cambridge: Cambridge University Press.

Bouquet, A., Glein, C. R., Wyrick, D., & Waite, J. H. (2017). Alternative Energy: Production of H 2 by Radiolysis of Water in the Rocky Cores of Icy Bodies. *The Astrophysical Journal*, *840*(1), L8. doi: 10.3847/2041-8213/aa6d56

Bouquet, A., Mousis, O., Waite, J. H., & Picaud, S. (2015). Possible evidence for a methane source in Enceladus' ocean. *Geophysical Research Letters*, *42*(5), 1334–1339. doi: 10.1002/2014GL063013

Bradley, J. A., Arndt, S., Amend, J. P., Burwicz, E., Dale, A. W., Egger, M., & LaRowe, D. E. (2020). Widespread energy limitation to life in global subseafloor sediments. *Science Advances*, *6*(32), eaba0697. doi: 10.1126/sciadv.aba0697

Brazelton, W. J., Schrenk, M. O., Kelley, D. S., & Baross, J. A. (2006). Methane- and sulfur-metabolizing microbial communities dominate the lost city hydrothermal field ecosystem. *Applied and Environmental Microbiology*, *72*(9), 6257-6270. doi: 10.1128/AEM.00574-06

Cable, M. L., Neveu, M., Hsu, H. W., & Hoehler, T. M. (2020). Enceladus. In V. S. Meadows, D. J. Des Marais, G. N. Arney, & B. E. Schmidt (Eds.), *Planetary Astrobiology* (pp. 217–246). Tucson, AZ: University of Arizona Press.

Cable, M. L., Porco, C., Glein, C. R., German, C. R., MacKenzie, S. M., Neveu, M., ... Núñez, J. (2021). The Science Case for a Return to Enceladus. *The Planetary Science Journal*, *2*(4), 132. doi: 10.3847/PSJ/abfb7a

Choblet, G., Tobie, G., Sotin, C., Běhounková, M., Čadek, O., Postberg, F., & Souček, O. (2017). Powering prolonged hydrothermal activity inside Enceladus. *Nature Astronomy*, *1*(12), 841–847. doi: 10.1038/s41550-017-0289-8

Cockell, C. S. (2011). Vacant habitats in the Universe. *Trends in Ecology & Evolution*, *26*(2), 73–80. doi: 10.1016/j.tree.2010.11.004

Cockell, C. S., Wordsworth, R., Whiteford, N., & Higgins, P. M. (2021). Minimum Units of Habitability and Their Abundance in the Universe. *Astrobiology*, *21*(4), 481–489. doi: 10.1089/ast.2020.2350

Cowan, D. A. (2004). The upper temperature for life–where do we draw the line? *Trends in microbiology*, *12*(2), 58–60. doi: 10.1016/j.tim.2003.12.002

Glein, C. R., Baross, J. A., & Waite, J. H. (2015). The pH of Enceladus' ocean.

Geochimica et Cosmochimica Acta, *162*, 202–219. doi: 10.1016/j.gca.2015.04.017

Glein, C. R., Postberg, F., & Vance, S. D. (2018). The Geochemistry of Enceladus: Composition and Controls. In P. M. Schenk, R. N. Clark, C. J. A. Howett, A. J. Verbiscer, & J. H. Waite (Eds.), *Enceladus and the Icy Moons of Saturn* (pp. 39–56). Tucson, AZ: University of Arizona Press. doi: 10.2458/azu_uapress_9780816537075-ch003

Glein, C. R., & Waite, J. H. (2020). The Carbonate Geochemistry of Enceladus' Ocean. *Geophysical Research Letters*, *47*(3), e2019GL085885. doi: 10.1029/2019GL085885

Hand, K. P., Sotin, C., Hayes, A., & Coustenis, A. (2020). On the Habitability and Future Exploration of Ocean Worlds. *Space Science Reviews*, *216*(5), 95. doi: 10.1007/s11214-020-00713-7

Harrison, J. P., Gheeraert, N., Tsigelnitskiy, D., & Cockell, C. S. (2013). The limits for life under multiple extremes. *Trends in Microbiology*, *21*(4), 204 – 212. doi: 10.1016/j.tim.2013.01.006

Hemingway, D. J., & Mittal, T. (2019). Enceladus's ice shell structure as a window on internal heat production. *Icarus*, *332*, 111–131. doi: 10.1016/j.icarus.2019.03.011

Hendrix, A. R., Hurford, T. A., Barge, L. M., Bland, M. T., Bowman, J. S., Brinckerhoff, W., ... Vance, S. D. (2018). The NASA Roadmap to Ocean Worlds. *Astrobiology*, *19*(1), 1–27. doi: 10.1089/ast.2018.1955

Higgins, P. M. (2021). *Nutmeg.* (Python package available at https://github.com/pmhiggins/NutMEG) doi: 10.5281/zenodo.4746771

Higgins, P. M., & Cockell, C. S. (2020). A bioenergetic model to predict habitability, biomass and biosignatures in astrobiology and extreme conditions. *Journal of The Royal Society Interface*, *17*(171), 20200588. doi: 10.1098/rsif.2020.0588

Hoehler, T. M. (2004). Biological energy requirements as quantitative boundary conditions for life in the subsurface. *Geobiology*, *2*(4), 205–215. doi: https://doi.org/10.1111/j.1472-4677.2004.00033.x

Hoehler, T. M. (2007). An Energy Balance Concept for Habitability. *Astrobiology*, *7*(6), 824–838. doi: 10.1089/ast.2006.0095

Hoehler, T. M., & Jørgensen, B. B. (2013). Microbial life under extreme energy limitation. *Nature Reviews Microbiology*, *11*(2), 83–94. doi: 10.1038/nrmicro2939

Hsu, H.-W., Postberg, F., Sekine, Y., Shibuya, T., Kempf, S., Horányi, M., ... others (2015). Ongoing hydrothermal activities within Enceladus. *Nature*, *519*(7542), 207–210. doi: 10.1038/nature14262

Iess, L., Stevenson, D. J., Parisi, M., Hemingway, D., Jacobson, R. A., Lunine, J. I., ... Tortora, P. (2014). The Gravity Field and Interior Structure of Enceladus. *Science*, *344*(6179), 78–80. doi: 10.1126/science.1250551

Jin, Q., & Bethke, C. M. (2007). The thermodynamics and kinetics of microbial metabolism. *American Journal of Science*, *307*(4), 643–677. doi: 10.2475/04.2007.01

Johnson, J. W., Oelkers, E. H., & Helgeson, H. C. (1992). SUPCRT92: A software package for calculating the standard molal thermodynamic properties of minerals, gases, aqueous species, and reactions from 1 to 5000 bar and 0 to 1000 C. *Computers & Geosciences*, *18*(7), 899–947. doi: 10.1016/0098-3004(92)90029-Q

Jones, R. M., Goordial, J. M., & Orcutt, B. N. (2018). Low Energy Subsurface Environments as Extraterrestrial Analogs. *Frontiers in Microbiology*, *9*. doi: 10.3389/fmicb.2018.01605

Khawaja, N., Postberg, F., Hillier, J., Klenner, F., Kempf, S., Nölle, L., ... Srama, R. (2019). Low-mass nitrogen-, oxygen-bearing, and aromatic compounds in Enceladean ice grains. *Monthly Notices of the Royal Astronomical Society*, *489*(4), 5231–5243. doi: 10.1093/mnras/stz2280

Kulp, T., Han, S., Saltikov, C., Lanoil, B., Zargar, K., & Oremland, R. (2007). Effects of imposed salinity gradients on dissimilatory arsenate reduction, sulfate reduction, and other microbial processes in sediments from two california soda lakes. *Applied and environmental microbiology*, *73*(16), 5130–5137.

LaRowe, D. E., & Helgeson, H. C. (2006). Biomolecules in hydrothermal systems: Calculation of the standard molal thermodynamic properties of nucleic-acid bases, nucleosides, and nucleotides at elevated temperatures and pressures. *Geochimica et Cosmochimica Acta*, *70*(18), 4680–4724. doi: 10.1016/j.gca.2006.04.010

Lauro, F. M., & Bartlett, D. H. (2008). Prokaryotic lifestyles in deep sea habitats. *Extremophiles*, *12*(1), 15–25. doi: 10.1007/s00792-006-0059-5

Lever, M. A., Rogers, K. L., Lloyd, K. G., Overmann, J., Schink, B., Thauer, R. K., ... Jørgensen, B. B. (2015). Life under extreme energy limitation: a synthesis of laboratory- and field-based investigations. *FEMS Microbiology Reviews*, *39*(5), 688–728. doi: 10.1093/femsre/fuv020

Liao, Y., Nimmo, F., & Neufeld, J. A. (2020). Heat Production and Tidally Driven Fluid Flow in the Permeable Core of Enceladus. *Journal of Geophysical Research: Planets*, *125*(9), e2019JE006209. doi: https://doi.org/10.1029/2019JE006209

Lingam, M., & Loeb, A. (2018). Is Extraterrestrial Life Suppressed on Subsurface Ocean Worlds due to the Paucity of Bioessential Elements? *The Astronomical Journal*, *156*(4), 151. doi: 10.3847/1538-3881/aada02

Lobo, A. H., Thompson, A. F., Vance, S. D., & Tharimena, S. (2021). A pole-to-equator ocean overturning circulation on Enceladus. *Nature Geoscience*, *14*(4), 185–189. doi: 10.1038/s41561-021-00706-3

MacKenzie, S. M., Neveu, M., Davila, A. F., Lunine, J. I., Craft, K. L., Cable, M. L., ... Spilker, L. J. (2021). The Enceladus Orbilander Mission Concept: Balancing Return and Resources in the Search for Life. *The Planetary Science Journal*, *2*(2), 77. doi: 10.3847/PSJ/abe4da

Magee, B. A., & Waite, J. H. (2017). Neutral Gas Composition of Enceladus' Plume — Model Parameter Insights from Cassini-INMS. *Lunar and Planetary Science Conference Abstract*. Retrieved from `https://www.hou.usra.edu/meetings/lpsc2017/pdf/2974.pdf`

McDermott, J. M., Sylva, S. P., Ono, S., German, C. R., & Seewald, J. S. (2020). Abiotic redox reactions in hydrothermal mixing zones: Decreased energy availability for the subsurface biosphere. *Proceedings of the National Academy of Sciences*, *117*(34), 20453–20461. doi: 10.1073/pnas.2003108117

McGenity, T. J. (2010). Methanogens and methanogenesis in hypersaline environments. In K. Timmis, T. McGenity, J. van der Meer, & V. de Lorenzo (Eds.), *Handbook of hydrocarbon and lipid microbiology* (pp. 665–680). Springer.

Meersman, F., Daniel, I., Bartlett, D. H., Winter, R., Hazael, R., & McMillan, P. F. (2013). High-Pressure Biochemistry and Biophysics. *Reviews in Mineralogy and Geochemistry*, *75*(1), 607–648. doi: 10.2138/rmg.2013.75.19

Mesbah, N. M., Cook, G. M., & Wiegel, J. (2009). The halophilic alkalithermophile natranaerobius thermophilus adapts to multiple environmental extremes using a large repertoire of na+ (k+)/h+ antiporters. *Molecular microbiology*, *74*(2), 270–281.

Nicholls, D. G., & Ferguson, S. J. (2013). 5 - Respiratory Chains. In D. G. Nicholls & S. J. Ferguson (Eds.), *Bioenergetics* (4th ed., pp. 91–157). Boston: Academic Press. doi: 10.1016/B978-0-12-388425-1.00005-1

Oren, A. (2011). Thermodynamic limits to microbial life at high salt concentrations. *Environmental microbiology*, *13*(8), 1908–1923. doi: 10.1111/j.1462-2920.2010.02365.x

O'Neill, C., & Nimmo, F. (2010). The role of episodic overturn in generating the surface geology and heat flow on Enceladus. *Nature Geoscience*, *3*(2), 88–91.

doi: 10.1038/ngeo731

Paranicas, C., Roussos, E., Krupp, N., Kollmann, P., Hendrix, A. R., Cassidy, T., ... Dialynas, K. (2012). Energetic charged particle weathering of Saturn's inner satellites. *Planetary and Space Science*, *61*(1), 60–65. doi: 10.1016/j.pss.2011.02.012

Plyasunov, A. V., & Shock, E. L. (2001). Correlation strategy for determining the parameters of the revised Helgeson-Kirkham-Flowers model for aqueous nonelectrolytes. *Geochimica et Cosmochimica Acta*, *65*(21), 3879–3900. doi: 10.1016/S0016-7037(01)00678-0

Postberg, F., Kempf, S., Schmidt, J., Brilliantov, N., Beinsen, A., Abel, B., ... Srama, R. (2009). Sodium salts in E-ring ice grains from an ocean below the surface of Enceladus. *Nature*, *459*(7250), 1098–1101. doi: 10.1038/nature08046

Postberg, F., Khawaja, N., Abel, B., Choblet, G., Glein, C. R., Gudipati, M. S., ... Waite, J. H. (2018). Macromolecular organic compounds from the depths of Enceladus. *Nature*, *558*(7711), 564–568. doi: 10.1038/s41586-018-0246-4

Ray, C., Glein, C. R., Hunter Waite, J., Teolis, B., Hoehler, T., Huber, J., ... Postberg, F. (2021). Oxidation processes diversify the metabolic menu on Enceladus. *Icarus*, 114248. doi: 10.1016/j.icarus.2020.114248

Sekine, Y., Shibuya, T., Postberg, F., Hsu, H.-W., Suzuki, K., Masaki, Y., ... Sirono, S.-i. (2015). High-temperature water–rock interactions and hydrothermal environments in the chondrite-like core of Enceladus. *Nature Communications*, *6*(1), 8604. doi: 10.1038/ncomms9604

Shock, E. L., Helgeson, H. C., & Sverjensky, D. A. (1989). Calculation of the thermodynamic and transport properties of aqueous species at high pressures and temperatures: Standard partial molal properties of inorganic neutral species. *Geochimica et Cosmochimica Acta*, *53*(9), 2157–2183. doi: 10.1016/0016-7037(89)90341-4

Smith, H. B., Drew, A., Malloy, J. F., & Walker, S. I. (2020). Seeding Biochemistry on Other Worlds: Enceladus as a Case Study. *Astrobiology*, *21*(2), 177–190. doi: 10.1089/ast.2019.2197

Smith, H. T., Shappirio, M., Johnson, R. E., Reisenfeld, D., Sittler, E. C., Crary, F. J., ... Young, D. T. (2008). Enceladus: A potential source of ammonia products and molecular nitrogen for Saturn's magnetosphere. *Journal of Geophysical Research: Space Physics*, *113*(A11). doi: https://doi.org/10.1029/2008JA013352

Steel, E. L., Davila, A., & McKay, C. P. (2017). Abiotic and Biotic Formation of Amino Acids in the Enceladus Ocean. *Astrobiology*, *17*(9), 862–875. doi: 10.1089/ast.2017.1673

Takai, K., Nakamura, K., Toki, T., Tsunogai, U., Miyazaki, M., Miyazaki, J., ... Horikoshi, K. (2008). Cell proliferation at 122 C and isotopically heavy CH4 production by a hyperthermophilic methanogen under high-pressure cultivation. *Proceedings of the National Academy of Sciences*, *105*(31), 10949–10954. doi: 10.1073/pnas.0712334105

Tan, S., Sekine, Y., Shibuya, T., Miyamoto, C., & Takahashi, Y. (2021). The role of hydrothermal sulfate reduction in the sulfur cycles within Europa: Laboratory experiments on sulfate reduction at 100 MPa. *Icarus*, *357*, 114222. doi: 10.1016/j.icarus.2020.114222

Taubner, R.-S., Pappenreiter, P., Zwicker, J., Smrzka, D., Pruckner, C., Kolar, P., ... Rittmann, S. K.-M. R. (2018). Biological methane production under putative Enceladus-like conditions. *Nature Communications*, *9*(1), 748. doi: 10.1038/s41467-018-02876-y

Taubner, R.-S., Schleper, C., Firneis, M. G., & Rittmann, S. K.-M. R. (2015). Assessing the Ecophysiology of Methanogens in the Context of Recent Astrobiological and Planetological Studies. *Life*, *5*(4), 1652–1686. doi:

10.3390/life5041652

Thauer, R. K., Jungermann, K., & Decker, K. (1977). Energy conservation in chemotrophic anaerobic bacteria. *Bacteriological reviews*, *41*(1), 100.

Thomas, P. C., Tajeddine, R., Tiscareno, M. S., Burns, J. A., Joseph, J., Loredo, T. J., ... Porco, C. (2016). Enceladus's measured physical libration requires a global subsurface ocean. *Icarus*, *264*, 37–47. doi: 10.1016/j.icarus.2015.08.037

Tijhuis, L., Van Loosdrecht, M. C., & Heijnen, J. J. (1993). A thermodynamically based correlation for maintenance gibbs energy requirements in aerobic and anaerobic chemotrophic growth. *Biotechnology and Bioengineering*, *42*(4), 509–519. doi: 10.1002/bit.260420415

Waite, J. H., Glein, C. R., Perryman, R. S., Teolis, B. D., Magee, B. A., Miller, G., ... Bouquet, A. (2017). Cassini finds molecular hydrogen in the Enceladus plume: Evidence for hydrothermal processes. *Science*, *356*(6334), 155–159. doi: 10.1126/science.aai8703

Waite, J. H., Lewis, W. S., Magee, B. A., Lunine, J. I., McKinnon, W. B., Glein, C. R., ... Ip, W.-H. (2009). Liquid water on Enceladus from observations of ammonia and ^{40}Ar in the plume. *Nature*, *460*(7254), 487–490. doi: 10.1038/nature08153

Wheat, C. G., Fisher, A. T., McManus, J., Hulme, S. M., & Orcutt, B. N. (2017). Cool seafloor hydrothermal springs reveal global geochemical fluxes. *Earth and Planetary Science Letters*, *476*, 179–188. doi: 10.1016/j.epsl.2017.07.049

Worman, S. L., Pratson, L. F., Karson, J. A., & Schlesinger, W. H. (2020). Abiotic hydrogen (H2) sources and sinks near the Mid-Ocean Ridge (MOR) with implications for the subseafloor biosphere. *Proceedings of the National Academy of Sciences*, *117*(24), 13283–13293. doi: 10.1073/pnas.2002619117

Zandanel, A., Truche, L., Hellmann, R., Myagkiy, A., Choblet, G., & Tobie, G. (2021). Short lifespans of serpentinization in the rocky core of Enceladus: Implications for hydrogen production. *Icarus*, *364*, 114461. doi: 10.1016/j.icarus.2021.114461

Zolotov, M. Y. (2007). An oceanic composition on early and today's Enceladus. *Geophysical Research Letters*, *34*(23). doi: https://doi.org/10.1029/2007GL031234

Ćuk, M., Dones, L., & Nesvorný, D. (2016). Dynamical evidence for a late formation of saturn's moons. *The Astrophysical Journal*, *820*(2), 97. doi: 10.3847/0004-637X/820/2/97